Physica B 486 (2016) 173–176

Contents lists available at ScienceDirect

Physica B

journal homepage: www.elsevier.com/locate/physb

Consistent energy barrier distributions in magnetic particle chains

O. Laslett [a,*], S. Ruta [b], R.W. Chantrell [b], J. Barker [c], G. Friedman [d], O. Hovorka [a]

[a] Engineering and the Environment, University of Southampton, Southampton, SO16 7QF, UK
[b] Department of Physics, University of York, York YO10 5DD, UK
[c] Institute for Materials Research, Tohoku University, Sendai 980-8577, Japan
[d] Electrical and Computer Engineering Department, Drexel University, Philadelphia, PA 19104, USA

ARTICLE INFO

Article history:
Received 16 June 2015
Received in revised form
7 September 2015
Accepted 22 September 2015
Available online 25 September 2015

Keywords:
Thermal relaxation
Energy barrier distributions
Magnetic particle chains
Dipolar interaction

ABSTRACT

We investigate long-time thermal activation behaviour in magnetic particle chains of variable length. Chains are modelled as Stoner–Wohlfarth particles coupled by dipolar interactions. Thermal activation is described as a hopping process over a multidimensional energy landscape using the discrete orientation model limit of the Landau–Lifshitz–Gilbert dynamics. The underlying master equation is solved by diagonalising the associated transition matrix, which allows the evaluation of distributions of time scales of intrinsic thermal activation modes and their energy representation. It is shown that as a result of the interaction dependence of these distributions, increasing the particle chain length can lead to acceleration or deceleration of the overall relaxation process depending on the initialisation procedure.

1. Introduction

A common feature in systems with hysteresis is a large number of metastable states leading to multiscale dynamics, ageing, and memory effects [1]. A phenomenological description of thermal activation processes in such systems assumes that the time scales τ of the available relaxation modes depend on the effective energy barriers, δe, emerging from internal interactions and disorder. Their probability distribution, $g_e(\delta e)$, is a characteristic of the system and its optimisation has been central to modern magnetic recording technology [2] and to applications of magnetic nanostructures in biology and medicine [3].

A standard way of identifying the energy barrier distribution $g_e(\delta e)$ has been based on the least square fitting of the integral expression:

$$M(t) = M_0 \int_0^\infty g_e(\delta e) e^{-t/\tau(\delta e)}\, \mathrm{d}(\delta e) \tag{1}$$

to the time dependent thermal relaxation magnetisation data [4]. Here M_0 is the initial magnetisation, $\tau(\delta e) = \tau_0 \exp(\delta e)$ following the Arrhenius law, and δe is assumed in the units of thermal energy k_BT. However, a recent study [5] demonstrated that the representation of thermal decay using Eq. (1) is inconsistent with the collective nature of thermally activated processes in interacting particle systems, and instead identified a consistent relation:

$$M(t) = M_0 \int_0^\infty f(\epsilon) e^{-t/\tau(\epsilon)}\, \mathrm{d}\epsilon \tag{2}$$

Here, the auxiliary variables ϵ are defined as $\tau(\epsilon) = \tau_0 \exp(\epsilon)$, where τ are the eigenmodes (reciprocals of eigenvalues) of the master equation associated with the discrete orientation model limit of the Landau–Lifshitz–Gilbert dynamics [5,6]. Thus $f(\epsilon)$ weights the contribution of a particular eigenmode τ, represented by $\epsilon = \ln(\tau/\tau_0)$, to the overall magnetisation decay at any time t. The variables ϵ have no direct physical meaning and have been introduced for convenience of comparing the eigenmodes with the energy scale of barriers δe, even though they have been found to reduce to δe in the non-interacting case or for geometrically symmetric particle clusters [5]. An equivalent formulation of Eq. (2) in terms of the intrinsic times τ can be obtained by substitution, which amounts to replacing $f(\epsilon)$ by $f(\ln(\tau/\tau_0))/\tau$ in the new integral over τ [7].

It is thus evident that the identification of the intrinsic properties of magnetic nanoparticles in the presence of interactions requires first relating $f(\epsilon)$ and $g_e(\delta e)$ in specific cases. Here we explore this issue for dipolar-coupled magnetic particle chains. This allows one to show that increasing the chain length can lead to acceleration or deceleration of thermal relaxation depending on the initialisation. The effect of initialisation on relaxation processes has been rarely addressed and cannot be explained based solely on the knowledge of $g_e(\delta e)$, as also suggested earlier [8].

* Corresponding author.
E-mail address: O.Laslett@soton.ac.uk (O. Laslett).

http://dx.doi.org/10.1016/j.physb.2015.09.044
0921-4526/

2. Method

A magnetic particle chain is modelled as a collection of interacting Stoner–Wohlfarth particles having spherical volume $V = \pi a^3/6$, where a is the particle diameter. Each particle is represented by a single macrospin unit vector $\hat{s}_i$ subject to anisotropy $\vec{k}_i = k_i\hat{k}_i$ and effective field $\vec{h} + \vec{h}_i^{\,\mathrm{dip}}$ as shown in Fig. 1(b), where $\vec{h}$ is the external applied field and $\vec{h}_i^{\,\mathrm{dip}}$ is the dipolar field produced by all neighbours of particle i. The total energy of a chain with N_s particles is

$$\frac{E}{V} = \sum_{i=0}^{N_s-1}\left(k_i\left(\hat{k}_i\times\hat{s}_i\right)^2 - \hat{s}_i\cdot\vec{h} - \hat{s}_i\cdot\vec{h}_i^{\,\mathrm{dip}}\right) \tag{3}$$

where $\vec{h}_i^{\,\mathrm{dip}} = I\sum_{j\neq i}^{N_s-1} r_{ij}^{-3}(-\hat{s}_j + 3\hat{r}_{ij}(\hat{s}_j\cdot\hat{r}_{ij}))$ is the dipolar interaction field with $\hat{r}_{ij} = \vec{r}_{ij}/r_{ij}$ and all distances normalised by a. The $I = \mu_0 M_s^2/24$ is the interaction strength and M_s the saturation magnetisation of the particles. The total system energy Eq. (3) has multiple minima that correspond to meta-stable states, referred to here as the microstates of the system and labeled $\alpha = 0, 1, \ldots, \Omega - 1$. For high energy barriers the system is confined to this set of discrete microstates and the thermally activated dynamics occur as a stochastic hopping process between these microstates. Fig. 1 (a) illustrates the 4 microstates corresponding to a 2-particle system, where the nodes and edges represent the microstates and possible transition paths of the system, respectively. In a constant magnetic field $\vec{h}$, each microstate α is representative of a specific particle moment configuration and has a definite magnetisation value m_α. The transition rates between each pair of microstates α, β are computed using the Néel–Arrhenius law that relates the energy barrier $\delta e_{\alpha\beta}$ between the microstates α and β to the transition rate: $W_{\alpha\beta} = \tau_0^{-1}\exp[-\delta e_{\alpha\beta}]$, where τ_0^{-1} is the attempt frequency (taken here constant $10^9\ \mathrm{s}^{-1}$), and $\delta e_{\alpha\beta}$ are in units of k_BT.

The probability that the system resides in a microstate α at a time t is denoted $p_\alpha(t)$. The time evolution of all microstate probabilities $\vec{p}(t)$ is studied by solving the master equation [9,10] motivated by the discrete orientation model limit of the Landau–Lifshitz–Gilbert dynamics [6]:

$$\frac{d}{dt}\vec{p}(t) = W\vec{p}(t) \tag{4}$$

with W being the $\Omega\times\Omega$ transition matrix. The matrix elements $W_{\alpha\beta}$ correspond to the Arrhenius transition rates from microstate β to α. In a constant external magnetic field, Eq. (4) represents a system of linear first-order differential equations subject to an initial condition $\vec{p}(0)$, and the general solution can be expressed by diagonalisation of the transition matrix [5,9], yielding the time evolution of the probability of each state as

$$p_\alpha(t) = \sum_{r=0}^{\Omega-1} c_r u_r^\alpha e^{-\lambda_r t} \tag{5}$$

In Eq. (5), $\lambda_r > 0$ are the eigenvalues of the transition matrix W relating to thermal activation modes with time scales $\tau_r = 1/\lambda_r$, u_r^α are the components of the right eigenvectors of W, and c_r are constants specified by the initial condition $\vec{p}(0)$. The overall time dependent magnetisation for a chain is $M_q(t) = \sum_\alpha m_\alpha p_\alpha(t)$, which after inserting Eq. (5) and arranging gives

$$M_q(t) = \sum_{\alpha=0}^{\Omega-1}\sum_{r=0}^{\Omega-1} m_\alpha c_r u_r^\alpha e^{-\lambda_r t} = \sum_{r=0}^{\Omega-1}\xi_r e^{-\lambda_r t} \tag{6}$$

where $\xi_r = \sum_\alpha c_r m_\alpha u_r^\alpha$ are the weights of the contribution of relaxation modes τ_r to the overall magnetisation decay of a chain. For convenience, we define the energy representation ϵ_r of the relaxation modes τ_r as $\tau_r = \tau_0\exp(\epsilon_r)$, which reduces to energy barriers $(\delta e_{\alpha\beta} + \delta e_{\beta\alpha})/2$ in the non-interacting case. Eq. (6) resembles the form of Eq. (2) for a single particle chain.

To apply this formalism one must first identify all applicable microstates α, energy barriers $\delta e_{\alpha\beta}$, and the transition rates $W_{\alpha\beta}$, which soon becomes a nontrivial numerical minimisation problem as the number of particles N_s in a chain increases. An algorithm to achieve this in the weakly interacting case has been discussed in [5], where the assumption of weak interactions allowed the consideration of single particle transitions only, and approximation of the $\delta e_{\alpha\beta}$ underlying these transitions by single particle Stoner–Wohlfarth-like effective barriers.

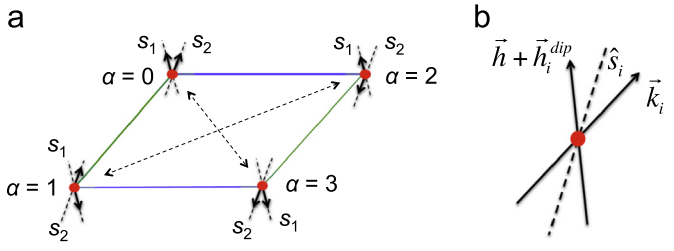

Fig. 1. (a) An example of a transition network in the state-space $\alpha = 0, \ldots 3$ of a 2-particle system $\hat{s}_1$ and $\hat{s}_2$. Thick arrows indicate the particle moment orientations within the microstates α. The edges along the perimeter of the network describe 'single-particle' transitions, the diagonal edges show transitions when both particle moments reorient simultaneously. (b) Stable particle moments $\hat{s}_i$ correspond to energy minima in Eq. (3), and are confined in the plane defined by the anisotropy vector $\hat{k}_i$ and the total local (effective) field $\vec{h} + \vec{h}_i^{\,\mathrm{dip}}$.

3. System of two interacting particles

We demonstrate the concepts developed above by considering a 2-particle example. In the weakly interacting case in zero field $\vec{h} = 0$ we expect each particle to exhibit two states, which leads to $2^2 = 4$ system microstates (Fig. 1(a)), and the likelihood of only single particle transitions. The most general form of the matrix W is in this case:

$$W = \begin{pmatrix} -\sum_0 & w_{01} & w_{02} & 0 \\ w_{10} & -\sum_1 & 0 & w_{13} \\ w_{20} & 0 & -\sum_2 & w_{23} \\ 0 & w_{31} & w_{32} & -\sum_3 \end{pmatrix} \tag{7}$$

where $\sum_i$ correspond to the sum of all elements in the column i. Calculating the eigenvalues of the matrix W, in order to set up Eq. (6), requires employing standard numerical methods.

For two identical particles with aligned anisotropy axes differing only by the anisotropy value k_i, it can be shown by straightforward symmetry arguments that $w_{01} = w_{32} = w_a$, $w_{10} = w_{23} = w_b$, $w_{20} = w_{13} = w_c$, and $w_{31} = w_{02} = w_d$. In this case, the eigenvalues can be calculated in closed form:

$$\lambda_1 = 0, \quad \lambda_2 = w,$$
$$\lambda_{3,4} = \frac{1}{2}\left(w \pm \sqrt{w^2 - (w_a w_c + w_b w_d)}\right) \tag{8}$$

with $w = w_a + w_b + w_c + w_d$. As can be seen, λ_1 corresponds to the thermodynamic equilibrium and λ_2 is simply a superposition of the relaxation rates evaluated directly from the energy barriers $\delta e_{\alpha\beta}$. However, λ_3 and λ_4 are nonlinear combinations of the transition rates $w_a, \ldots, w_d$, which complicates identification of their relation to $\delta e_{\alpha\beta}$ unless the functional form of the non-linear

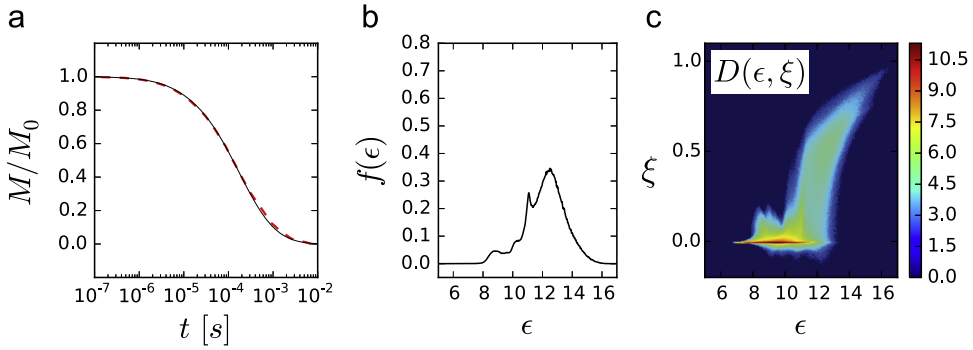

Fig. 2. (a) The time-dependent magnetisation $M(t)$ for 10^6 4-particle chains as computed with Eq. (2) (–) using the normalised distribution $f(\epsilon)$ shown in (b). The histogram representing the joint probability density function $D(\epsilon, \xi)$ used to compute $f(\epsilon)$ in Eq. (10) is shown in (c). In (a), the dashed line (– –) correspond to equivalent kinetic Monte Carlo simulations. The model parameters used are discussed in the text.

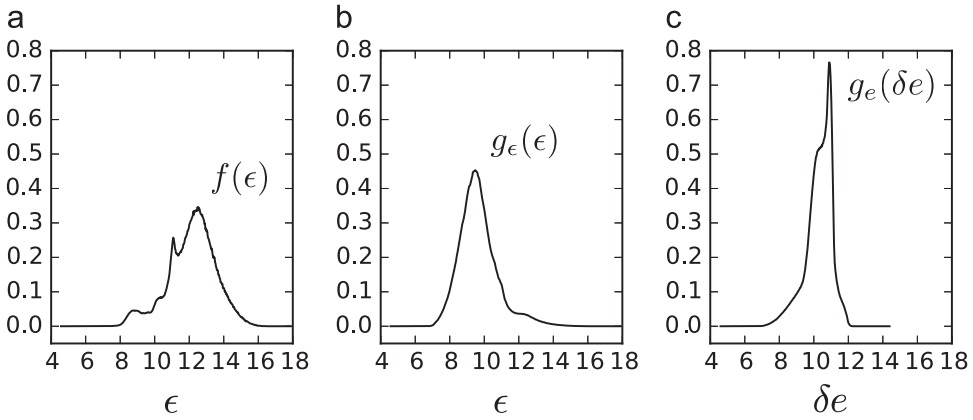

Fig. 3. An example of the computed normalised probability distribution $f(\epsilon)$ for an ensemble of 4-particle chains initialised in an external field oriented parallel to the chain axis. For comparison, (b) shows the probability distribution g_ϵ of ϵ obtained directly as eigenvalues of the transition matrix W, and (c) the distribution g_e of energy barriers δe obtained by the direct minimisation of Eq. (3).

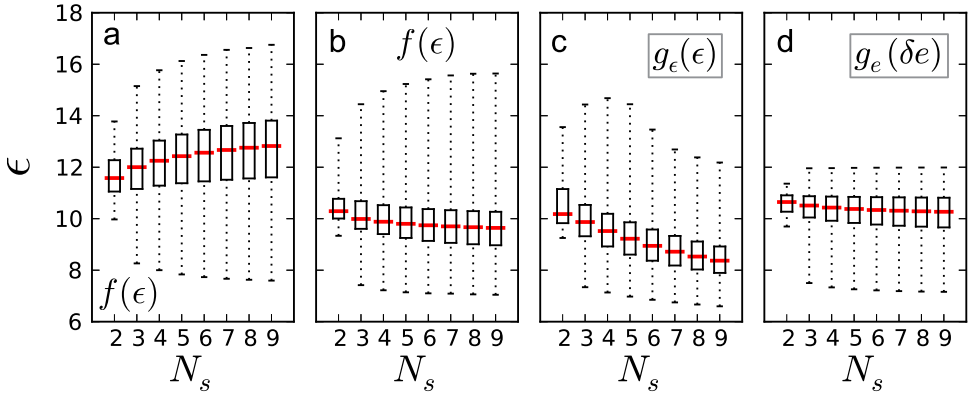

Fig. 4. Box-and-whisker plots of the different types of distributions computed for particle chains of length N_s. The 'box' corresponds to lower and upper quartiles of the distribution, and the lower and upper 'whiskers' mark the tails of the distribution. The horizontal line through the box is the median. (a)-(b) $f(\epsilon)$ corresponding to initialisation of a thermally activated process in external field parallel (a) and perpendicular (b) with respect to the chain axis. (c) Distribution $g_\epsilon(\epsilon)$ obtained directly from the eigenvalues of the transition matrix W, and (d) distribution $g_e(\delta e)$ of energy barriers obtained by the direct minimisation of the energy function Eq. (3).

dependence is known. Such information is only rarely available in practice.

The next level of reduction is to consider two identical interacting particles. The higher level of symmetry simplifies the W matrix even further with $w_b = w_c = w_0$ and $w_a = w_d = w_1$, the corresponding eigenvalues are

$$\lambda_1 = 0, \quad \lambda_2 = 2(w_0 + w_1),$$
$$\lambda_{3,4} = w_0 + w_1 \pm |w_0 - w_1| \tag{9}$$

This case also allows identification of the energy barriers by minimisation of the full energy expression (Eq. (3)): $\delta e_0 = kV/k_BT((1-2I^*)^2 - I^{*2})$ and $\delta e_1 = kV/k_BT((1+2I^*)^2 - I^{*2})$, where $I^* = I/(2k)$ with I being the interaction strength entering in the dipolar term in Eq. (3), and $k = |\vec{k}_i|$ for all particles.

Expressions (8) and (9) allow the calculation of the time and energy representations of the relaxation modes respectively as $\tau_r = 1/\lambda_r$ and $\epsilon_r = \ln(\tau_r/\tau_0)$. This in turn allows the evaluation of the microstate probability distribution in Eq. (5), the coefficients ξ_r, and ultimately the magnetisation decay using Eq. (6). The required microstate magnetisations m_α are obtained from direct minimisation of Eq. (3). In the following we apply these concepts to

investigate ensembles of particle chains with spherical distributions of anisotropy axes. Such chains require analysing general matrices, such as Eq. (7) for the 2-particle case, and employing numerical methods. Describing ensembles of chains also requires a statistical approach to be introduced below.

4. Ensembles of particle chains

In Figs. 2–4 we consider thermal relaxation behaviour in uniform ensembles of 10^6 independent chains of length $N_s = 2, \ldots, 9$, assuming zero external magnetic field and initialisation in the remanent state prepared by applying a saturating field parallel to the chain axis. For comparison, in Fig. 4(b) we have also included calculations for initialisation in a perpendicular magnetic field. As a simulation parameter set we use $a = 10$ nm, $T = 300$ K, spherically randomised anisotropies $\vec{k}_i$ with $k = |\vec{k}_i| = 10^7$ J/m^3 for all i, giving $kV/k_BT \approx 12.5$, and $M_s = 4 \times 10^5$ A/m which gives $I = 8.4 \times 10^3$ J/m^3. For every chain in the ensemble, we evaluate the eigenvalue problem and identify all quantities ξ_r and τ_r entering in Eq. (6), and find $\epsilon_r = \ln(\tau_r/\tau_0)$. Next, following Ref. [5], we use histogram techniques to find the joint probability distribution $D(\epsilon, \xi)$ corresponding to an ensemble of chains, and compute the distribution $f(\epsilon)$ entering in Eq. (2) as

$$f(\epsilon) = M_0^{-1} \int_{-\infty}^{\infty} \xi D(\epsilon, \xi)\, d\xi \tag{10}$$

An example of the calculation for an ensemble of 10^6 4-particle chains is shown in Fig. 2. In Fig. 2(a), the magnetisation decay is calculated using Eq. (2) assuming $f(\epsilon)$ shown in Fig. 2(b). The $f(\epsilon)$ was evaluated using Eq. (10) with $D(\epsilon, \xi)$ shown in Fig. 2(c), obtained as a normalised two dimensional histogram over all ξ and ϵ in the ensemble when they are viewed as correlated random variables. The distribution $D(\epsilon, \xi)$ provides a complete description of the thermally activated magnetisation decay behaviour of ensembles of chains. As can also be seen in Fig. 2(c), there is a dense ϵ region, approximately between $6 < \epsilon < 8$, where $\xi = 0$. According to Eq. (6), this region corresponds to those relaxation modes not contributing to the magnetisation decay, and relates to symmetric orientations of anisotropy axes of particles within the chains which are likely to be present in the ensemble.

Fig. 3 compares the distribution $f(\epsilon)$ for an ensemble of 4-particle chains (Fig. 3(a)), as already shown in Fig. 2(b), the corresponding full distribution of relaxation mode energies $g_\epsilon(\epsilon) = \int_{-\infty}^{\infty} D(\xi, \epsilon)\, d\xi$ (Fig. 3(b)), and the energy barrier distribution $g_e(\delta e)$ obtained by directly mapping the energy landscape (Fig. 3(c)). Clearly, $g_\epsilon(\epsilon)$ and $g_e(\delta e)$ have different functional form than $f(\epsilon)$, and while the distributions g_ϵ and g_e are intrinsic characteristics depending only on the complexity of the energy landscape, $f(\epsilon)$ reflects the nature of the measurement. For example, an equation analogous to Eq. (6) could in principle be derived for thermal fluctuations of the magnetic moment, which would lead to a different definition and functional profile for the distribution f, while the distributions g_ϵ and g_e would remain unchanged.

Fig. 4 shows a systematic study of the behaviour of distributions f, g_ϵ, and g_e for ensembles of particle chains of increasing length N_s, using box-and-whisker plots. The box corresponds to the lower and upper quartiles of the distribution and the whiskers mark the tails of the distribution (corresponding to 1% and 99% percentiles). The horizontal line through the box is the median. Fig. 4(a), (c), and (d) are analogous to Fig. 3, and are extended to include ensembles of chains with increasing N_s. As can be seen, the median of the distribution $f(\epsilon)$ moves upwards as N_s increases, which implies an increasing characteristic time scale of thermal relaxation during the approach to equilibrium, since increasing ϵ implies longer τ. It is also evident that the overall trend of distributions g_ϵ and g_e is markedly different from f. In Fig. 4(b) we also added the behaviour for ensembles of chains initialised in a different state obtained in perpendicular magnetic fields with respect to the chain axis. The trend as a function of N_s is markedly different, leading to accelerated relaxation. This highlights the importance of the initial condition in the overall relaxation process, as also discussed in [5] for more general cases of particle clusters.

5. Conclusions

We studied thermal relaxation behaviour in magnetic particle chains. Evaluating Eq. (2) we found that interactions can cause acceleration or deceleration of thermal relaxation process as the chain length increases depending on the initialisation. Our findings illustrate the rich behaviour of thermally activated processes in interacting particle systems, which may be completely missed if the analysis is based on the energy barrier distributions $g_e(\delta e)$, as is often done in practice. Because $g_e(\delta e)$ relate to the overall topography of the energy landscape, they inherently cannot account for the initialisation dependent thermally activated hopping processes and, therefore, cannot be directly used to quantify the magnetisation decay behaviour. Thus, fundamentally, the inverse problems to identify intrinsic properties of interacting magnetic particle systems are ill-posed, unless the initialisation procedure is included in the analysis through consistent evaluation of thermal activation modes.

Acknowledgements

We gratefully acknowledge financial support from the EPSRC doctoral training centre grant (EP/G03690X/1).

References

[1] G. Bertotti, I.D. Mayergoyz, The Science of Hysteresis: Physical modeling, micromagnetics, and magnetization dynamics, vol. 2, Elsevier, Oxford, 2006.
[2] S. Piramanayagam, K. Srinivasan, Recording media research for future hard disk drives, J. Magn. Magn. Mater. 321 (2009) 485–494.
[3] Q.A. Pankhurst, J. Connolly, S. Jones, J. Dobson, Applications of magnetic nanoparticles in biomedicine, J. Phys. D: Appl. Phys. 36 (2003) R167.
[4] R. Kodama, Magnetic nanoparticles, J. Magn. Magn. Mater. 200 (1999) 359–372.
[5] O. Hovorka, J. Barker, G. Friedman, R.W. Chantrell, Role of geometrical symmetry in thermally activated processes in clusters of interacting dipolar moments, Phys. Rev. B 89 (2014) 104410.
[6] W.F. Brown Jr., Thermal fluctuation of fine ferromagnetic particles, IEEE Trans. Magn. 15 (1979) 1196–1208.
[7] O. Laslett, S. Ruta, J. Barker, R. Chantrell, G. Friedman, O. Hovorka, Interaction effects enhancing magnetic particle detection based on magneto-relaxometry, Appl. Phys. Lett. 106 (2015) 012407.
[8] O. Iglesias, A. Labarta, Magnetic relaxation in terms of microscopic energy barriers in a model of dipolar interacting nanoparticles, Phys. Rev. B 70 (2004) 144401.
[9] J. Schnakenberg, Network theory of microscopic and macroscopic behavior of master equation systems, Rev. Mod. Phys. 48 (1976) 571–585.
[10] I. Klik, C.-R. Chang, Thermal relaxation in arrays of coupled ferromagnetic particles, Phys. Rev. B 52 (1995) 3540–3545.